



STRUCTURAL
BIOLOGY

Volume 78 (2022)

Supporting information for article:

A new inactive conformation of SARS-CoV-2 main protease

Emanuele Fornasier, Maria Ludovica Macchia, Gabriele Giachin, Alice Sobic, Matteo Pavan, Mattia Sturlese, Cristiano Salata, Stefano Moro, Barbara Gatto, Massimo Bellanda and Roberto Battistutta

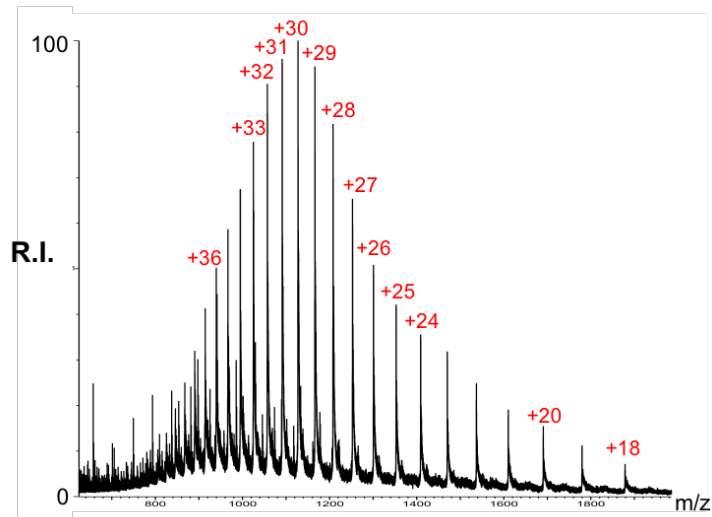


Figure S1

ESI-MS spectrum of full-length recombinant SARS-CoV-2 M^{pro} (residues 1-306). The sample containing 2 μ M of the recombinant full-length SARS-CoV-2 M^{pro} was analyzed in 50% acetonitrile added of 0.1% formic acid in positive ion mode by direct infusion ESI-MS. For the sake of clarity, only a few charge states of the detected species are reported in the Figure. The species displayed a deconvoluted mass of 33796.64 Da vs a calculated one of 33796.81 Da.

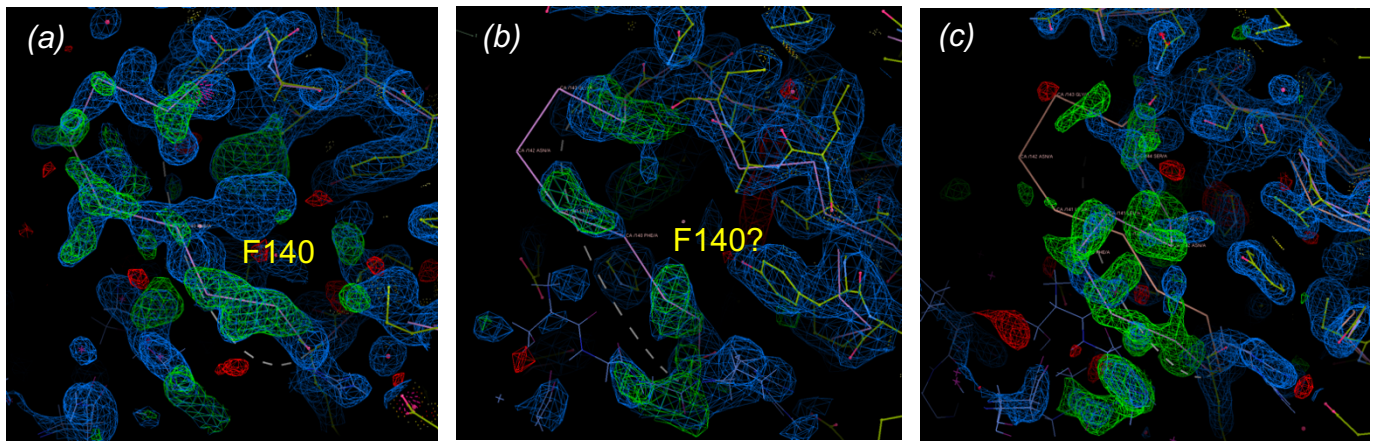


Figure S2

Initial electron densities. Representative situations after MR and a first step of refinement using a model lacking residues 139-144, 1-3 and with H163A substitution (see methods for details). Panel (a), M^{pro} with good density of the oxyanion loop in the active conformation ($C\alpha$ trace in magenta); side chains are visible, in particular for Phe140. Panel (b), M^{pro} with very poor density for the oxyanion loop; no densities for side chains are visible. Panel (c), M^{pro} electron densities clearly indicate a different conformation for the oxyanion loop (in orange the trace for the active conformation, in magenta the trace for the new conformation, new-inactive M^{pro}). $2F_o-F_c$ maps in blue (contour level 1.0σ), F_o-F_c maps in green/red (contour level 3.0σ). The white dashed line indicates the missing 139-144 residues.

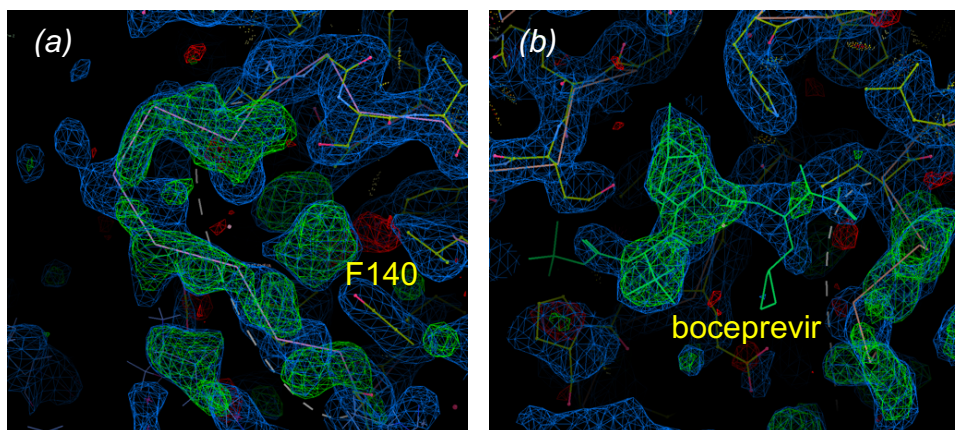


Figure S3

Initial electron densities for the M^{pro} /boceprevir complex. Representative situations after MR and a first step of refinement using a model lacking residues 139-144 and 1-3, with H163A substitution and without boceprevir (see methods for details). Panel (a), M^{pro} with good density of the oxyanion loop in the active conformation ($C\alpha$ trace in magenta); side chains are visible, in particular for Phe140. Panel (b), electron density indicating the presence of the inhibitor (the boceprevir molecule, still not present at this refinement stage, is shown for reference). $2F_o-F_c$ maps in blue (contour level 1.0σ), F_o-F_c maps in green/red (contour level 3.0σ). The white dashed line indicates the missing 139-144 residues.

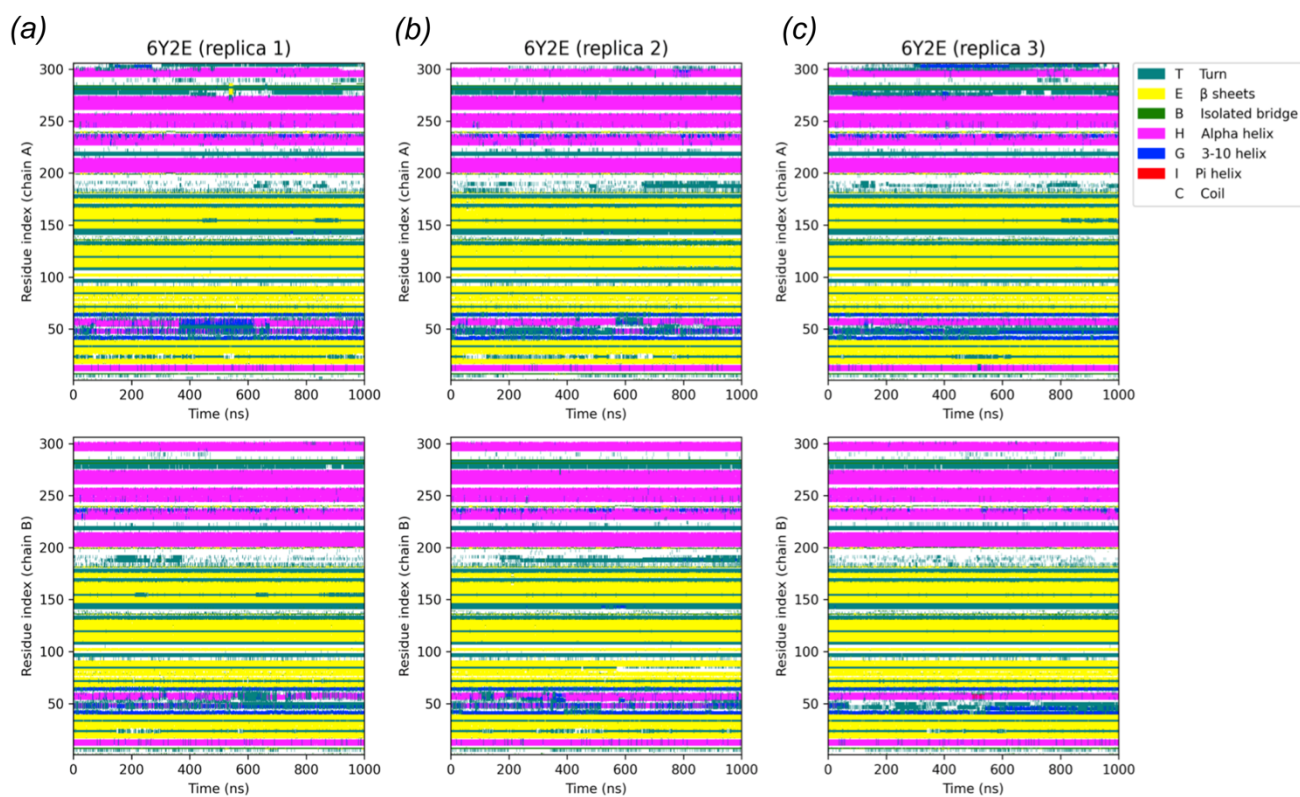


Figure S4

Time-dependent evolution of the secondary structure alongside the three MD simulations ((a), (b) and (c)) for protein 6Y2E (active conformation). Colors are arranged according to Visual Molecular Dynamics (VMD) convention, as depicted in the legend. Within each subpanel, data referring to chain A of the dimer is reported in the upper part, while data concerning chain B is reported in the lower one.

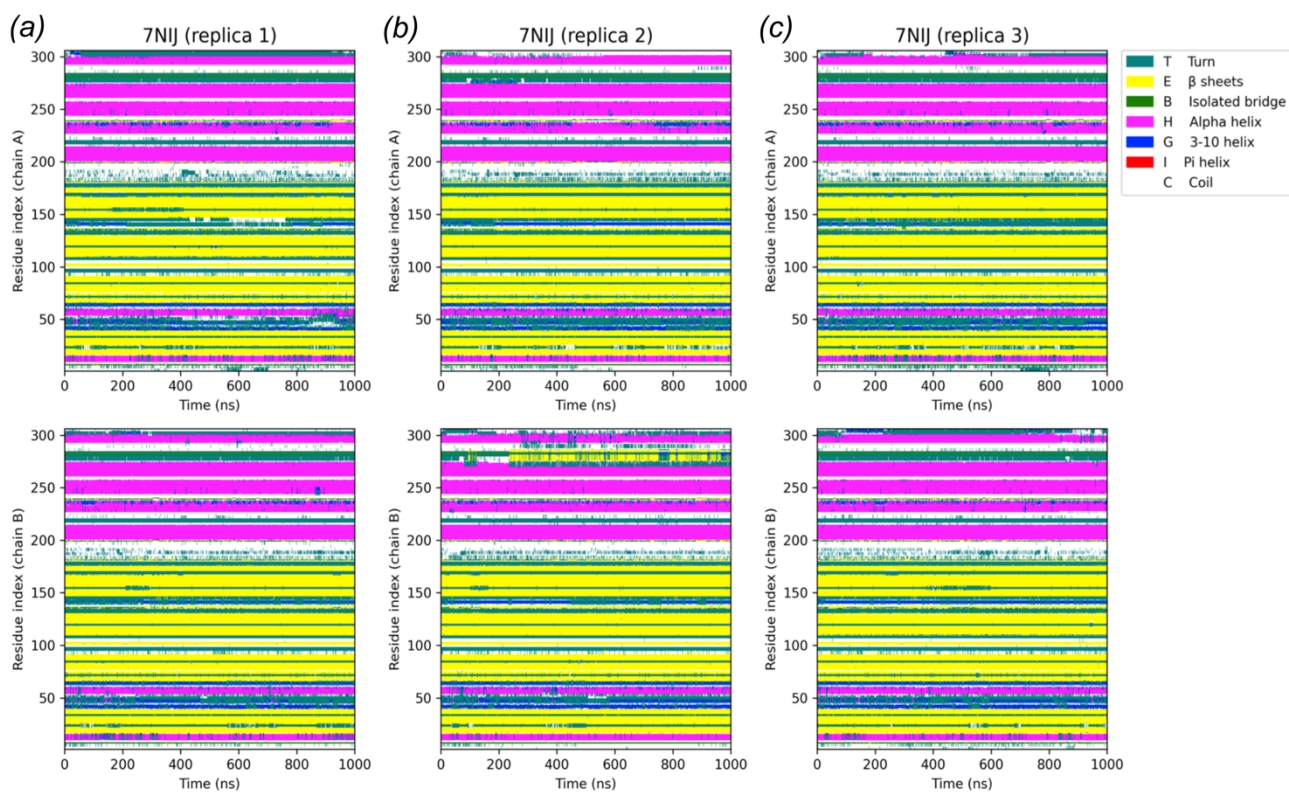


Figure S5

Time-dependent evolution of the secondary structure alongside the three MD simulations ((a), (b) and (c)) for protein 7NIJ (new-inactive). Colors are arranged according to Visual Molecular Dynamics (VMD) convention, as depicted in the legend. Within each subpanel, data referring to chain A of the dimer is reported in the upper part, while data concerning chain B is reported in the lower one.

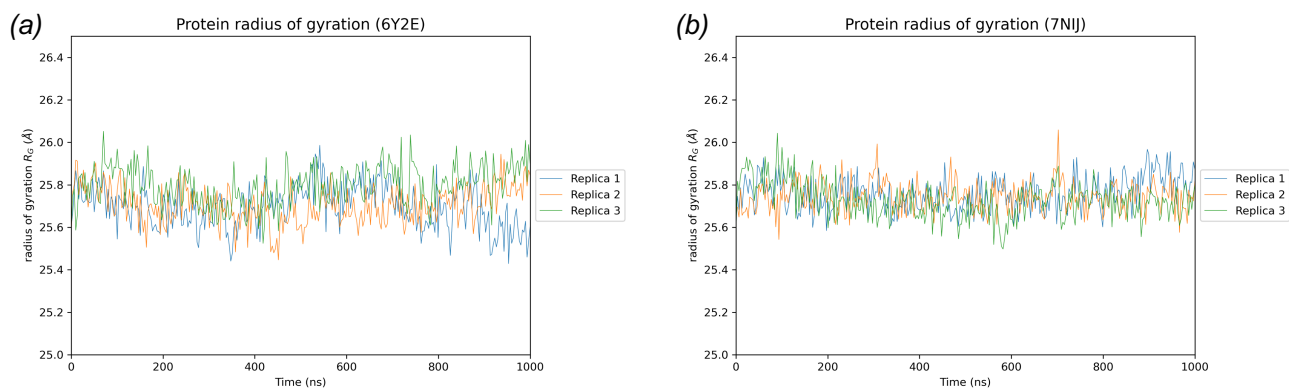


Figure S6

Time-dependent evolution of protein radius of gyration (R_g), for both the active (PDB ID: 6Y2E; panel (a)) and new-inactive (PDB ID: 7NIJ; panel (b)) conformations of SARS-CoV-2 M^{pro} .

Table S1

PDB codes and some significant pieces of information regarding the relevant structures of SARS-CoV-2 and SARS-CoV M^{Pro} discussed in the paper. We used 6Y2E as reference structure for ligand-free, active SARS-CoV-2 M^{Pro}. For recent comprehensive analyses of available SARS-CoV and SARS-CoV-2 M^{Pro} crystal structures see Behnam, 2021; Brzezinski et al., 2021; Jaskolski et al., 2021; Wlodawer et al., 2020.

*Structure 7NIJ is presented in this paper.

| PDB code | Coronavirus | Oxyanion loop conformation | Ligands | Mutations |
|----------|-------------|----------------------------|-------------------------------------|-----------|
| 7NIJ* | SARS-CoV-2 | new-inactive | no | no |
| 6Y2E | SARS-CoV-2 | active | no | no |
| 6M03 | SARS-CoV-2 | active | no | no |
| 5REL | SARS-CoV-2 | active | PCM-0102340 | no |
| 7K40 | SARS-CoV-2 | active | boceprevir | no |
| 2BX4 | SARS-CoV | active | no | no |
| 1UJ1-B | SARS-CoV | collapsed-inactive | no | no |
| 1UK2-B | SARS-CoV | collapsed-inactive | no | no |
| 2QCY | SARS-CoV | collapsed-inactive | no | R298A |
| 2Q6G | SARS-CoV | active | 11 _{mer} peptide substrate | no |
| 7KHP | SARS-CoV | active | C-terminal acyl-intermediate | no |

Table S2

Minimally frustrated energetic interactions involving selected amino acids of the active site in structure 6Y2E (“active”) and structure presented in this paper (“new-inactive”).

| | | 6Y2E | new-inactive |
|---------------|--------------|--------------|---------------------|
| Cys145 | Tyr25 | 0 | 0 |
| | Tyr26 | 0 | 0 |
| | Asn28 | 0 | - |
| | Gly29 | 0 | 0 |
| | Cys38 | 0 | 0 |
| | Val42 | 0 | 0 |
| | Cys117 | 0 | 0 |
| | Phe140 | 0 | - |
| | Gly143 | 0 | 0 |
| | Ser147 | 0 | 0 |
| | Met162 | 0 | 0 |
| | His163 | 0 | 0 |
| | His164 | 0 | 0 |
| | Met165 | 0 | 0 |
| | Glu166 | 0 | - |
| | Gly174 | 0 | 0 |
| | Total | 16 | 13 |
| Phe140 | Val114 | 0 | - |
| | Ala116 | 0 | - |
| | Ile138 | 0 | - |
| | Cys145 | 0 | - |
| | His163 | 0 | - |
| | Met165 | 0 | - |
| | Glu166 | 0 | - |
| | His172 | 0 | - |
| | | Total | 8 |
| Cys117 | Val13 | 0 | - |
| | Glu14 | - | 0 |
| | Met17 | - | 0 |
| | Val18 | 0 | 0 |
| | Gln19 | 0 | 0 |
| | Leu27 | - | 0 |
| | Gly29 | - | 0 |
| | Val114 | 0 | 0 |
| | Leu15 | 0 | 0 |
| | Asn119 | - | 0 |
| | Gly120 | 0 | 0 |
| | Pro122 | - | 0 |
| | Ser123 | - | 0 |
| | Leu41 | - | 0 |
| | Gly143 | - | 0 |
| | Ser144 | 0 | 0 |
| | Cys145 | 0 | 0 |
| | Ser147 | 0 | 0 |
| | Val148 | 0 | 0 |
| | Total | 10 | 18 |
| Leu141 | Ala116 | - | 0 |
| | Cys117 | - | 0 |
| Gly143 | Cys117 | - | 0 |
| | Tyr118 | 0 | - |
| | Gly138 | - | 0 |
| Ser144 | Cys145 | 0 | 0 |
| | Cys117 | 0 | 0 |
| | Total | 3 | 6 |